



NUMERICAL SIMULATION OF VELOCITY FLUCTUATIONS AND DISPERSION OF SEDIMENTATING PARTICLES

F. R. CUNHA
A. J. SOUSA

Department of Mechanical Engineering,
University of Brasília, Brasília, Brazil

E. J. HINCH

Department of Applied Mathematics
and Theoretical Physics, University of Cambridge,
Cambridge, United Kingdom

Velocity fluctuations and hydrodynamic dispersion are studied in a mono-disperse dilute suspension of rigid spherical particles. In the absence of Brownian motion and inertia, fluctuations in the velocity of individual particles arise from hydrodynamic interactions varying with the ever-changing configurations of the particles. We show some computer simulations of point particles with excluded volume sedimenting in a rectangular container with periodic sides and impenetrable bottom and top. The simulations reproduce the experimental correlation-time and anisotropy of the velocity fluctuations but have a magnitude increasing proportionally to the size of the system.

Keywords: Hydrodynamic dispersion; Sedimentation; Fluctuations; Suspension; Point particles

Received 4 April 2000; in final form 13 March 2001.

Address correspondence to Francisco Ricardo Cunha, Department of Mechanical Engineering-FT, University of Brasília, Campus Universitário, 70910-900, Brasília-DF, Brazil.
Fax: 55-612734539

INTRODUCTION

Even if all the particles in a suspension are spheres of the same size and density, they will not all fall at the same velocity. The hydrodynamic interactions depend on the relative location of neighboring particles. Thus in a random suspension, particles in different configurations will fall at different velocities. These differing velocities will in turn change the configurations, so the velocity of each particle will also vary in time. This random motion of the particles can at longer times be characterized by a self-induced hydrodynamic diffusivity. This dispersion phenomenon is important for understanding mixing processes that reduce separation (Davis, 1996).

The origin, significance, and interpretation of the convergence difficulties in calculating the sedimentation velocity in a random monodisperse dilute suspension are now well understood after Batchelor (1972). However, a dramatic illustration of the convergence problem in such suspensions is given by the divergence of the variance of the sedimentation velocity, $\langle U'^2 \rangle$, the simplest measure of the particle velocity fluctuations. This paradoxical situation was first noticed by Caffisch and Luke (1985), who showed that Batchelor's renormalization does not resolve the divergence associated with calculating the variance of the sedimentation velocity. Indeed, they found that the variance of the particle velocity in a monodisperse suspension of spheres whose the positions were randomly distributed with uniform probability would increase with the linear dimension ℓ of the container, i.e., the variance would be $O(U_s^2 \phi \ell / a)$, where $U_s = 2\Delta\rho a^2 g / 9\mu$ is the Stokes velocity for an isolated particle, a is the particle radius, $\Delta\rho$ denotes the difference between the density of the solid particles and the fluid, μ is the fluid viscosity, g is the acceleration due to gravity, and ϕ is the volume fraction of the dispersed phase. A scaling argument based on buoyancy-driven convection was proposed by Hinch (1988): volume elements of the suspension with lower density rising relative to volume elements with higher density (Cunha, 1997). The scalings confirmed the result of Caffisch and Luke (1985). Koch (1992) has adapted Hinch's scalings to gas-solid suspensions (i.e., dusty gas) and studied the behavior of fluctuations in a range of moderate Stokes number, $1 \ll St \ll \phi^{-3/4}$. His theory suggests that the velocity disturbance caused by neighboring particles is screened on a length scale $\chi = O(aSt^{-2/3}\phi^{-1})$, giving a finite variance of the particle velocity $\langle U'^2 \rangle = O(U_s^2 St^{-2/3})$. In addition, Koch (1993) has also investigated a dilute liquid-solid, slightly polydisperse suspension of spheres with $O(1)$ Reynolds number in which Oseen's equation was applicable. Here he predicted that although the resulting lift velocity is small compared to both the terminal velocity and the fluid velocity disturbance, it changes the structure of the suspension in a way to yield a screening length

$O(a\phi^{-1}p^{-1})$ and a finite velocity variance $O(U_s^2\phi \ln(1/p\phi))$, where p is a parameter much larger than one for a slightly polydisperse suspension.

Examining the convergence properties of the velocity variance in a sedimenting suspension with no inertia in the particles and fluid, Koch and Shaqfeh (1991) showed that the variance is independent of the size of the settling container if and only if the pair probability satisfies the criterion $\int[\mathcal{P}(\mathbf{x}|\mathbf{0}) - n]d\mathbf{x} = -1$, i.e., a test particle produces a net deficit of one particle in its neighborhood so that the combined unit of the test particle and its neighboring suspension is neutrally buoyant. This theory found a variance of the sedimentation velocity $\langle U'^2 \rangle = 4.7U_s^2$ and a dispersion coefficient parallel to gravity $D_{\parallel} = 0.52aU_s\phi^{-1}$ ($= 10.4aU_s$ at $\phi = 5\%$). Dynamical simulations of sedimenting particles with full hydrodynamic interaction in a periodic cubic system by Ladd (1993) and large-scale lattice-Boltzmann numerical simulations also by Ladd (1997) have shown, however, that the deficit is small and localized to the immediate vicinity of the spheres, and that at larger separations there is a net excess of neighbors.

Experiments have also been carried out to investigate fluctuations and dispersion during sedimentation. Davis and Hassen (1988) examined the spreading of the interface at the top of a sedimenting, slightly polydisperse suspension of non-Brownian particles. An investigation of the simultaneous effects of self-sharpening and velocity fluctuations in a sedimenting suspension of noncolloidal particles has been made by Lee et al. (1992). Ham and Homay (1988) carried out experiments to investigate the nature of the motion of a test particle sedimenting in the midst of a suspension of like particles. Their experiments found that fluctuations in the sedimentation velocity over relatively short settling distances are large (ranging from 25% to 46% of the mean) with dimensionless self-dispersion coefficients parallel to gravity increasing from approximately $2aU_s$ at $\phi = 25\%$ to $6aU_s$ at $\phi = 5\%$, which is about a factor of five smaller than the gradient diffusivity reported by Lee et al. (1992). Using a multiple light scattering technique, Xue et al. (1992) measured the effects of hydrodynamic interactions on the average sedimentation velocity, its variance, and the short-time self-diffusion coefficient in a concentrated hard-sphere colloidal suspension. The most recent experiments in sedimentation were carried out by Nicoali et al. (1995), who have also investigated velocity fluctuations and self-induced hydrodynamic dispersion in a monodisperse sedimenting suspension of non-Brownian spheres under conditions of low Reynolds number for dilute and higher particle concentration, $5\% \leq \phi \leq 40\%$. These experiments estimated velocity fluctuations between 75% and 170% of the mean, larger than those of Ham and Homay (1988), smaller, however, than the theoretical prediction $\sqrt{\langle U'^2 \rangle} = 2.2U_s$ of Koch and Shaqfeh (1991). In addition, they observed a strong anisotropy in the velocity fluctuations

and self-diffusivities, $D_{\parallel}/D_{\perp} \approx 5$ at 5%, although substantially smaller than that found by the theory of Koch (1994) and numerical simulations of Ladd (1993, 1997). At moderate concentration, Nicolai and Guazzelli (1995) found in contrast to the theories and computations, that particle velocity fluctuations and hydrodynamic self-dispersion coefficients did not depend on the container dimension, as the inner width of the vessel varied by a factor of four, and varied little with concentration in comparison to $\langle U \rangle$. At very low concentrations in a thin box, Ségre et al. (1997) found a $\phi^{1/3}$ dependence, and an independence of the wider of the horizontal dimensions if it exceeded a certain correlation length $\ell_c = 10a\phi^{-1/3}$. Curiously, this observed correlation length in the velocity fluctuations is somewhat greater than the narrower of the horizontal dimensions.

The experiments of Nicolai and Guazzelli (1995) unfortunately disagree with the theoretical predictions of Caffisch and Luke (1985) and Hinch (1988), which suggested a dependence of the velocity fluctuations on the system size. This contrary result may be an indication that a “well-stirred” particle distribution cannot, in principle, remained unchanged during sedimentation, and that information about the evolution of the microstructure in time is required to understand the behavior of the velocity fluctuations. Finally, we should mention the related phenomenon of shear-induced hydrodynamic diffusion for which diffusivities in sheared monodisperse suspensions of spheres have been determined experimentally (Leighton and Acrivos, 1987) and theoretically (Cunha and Hinch, 1996).

The aim of this article is to investigate by computer simulation the time dependence of the velocity fluctuations and dispersion as particles sediment. The important issue is to observe whether the suspension microstructure remains random and with uniform probability. To this end, we shall see how the positions of the spheres evolve in a finite container with impenetrable bottom and top and periodic sides.

ANALYSIS

Scaling Argument

One can begin to understand the scaling of the velocity fluctuations by considering a box of size ℓ containing N particles distributed uniformly, with the number of particles related to the size of the box and the volume fraction ϕ by $N = \ell^3 \phi / 4/3\pi a^3$. If the box is divided into two equal parts by a vertical plane (see Figure 1), due to statistical fluctuations one half of the box will typically contain $\frac{N}{2} + \sqrt{N}$ particles, whereas the other half will contain $\frac{N}{2} - \sqrt{N}$. This imbalance drives convection currents during the sedimentation process. The extra weight

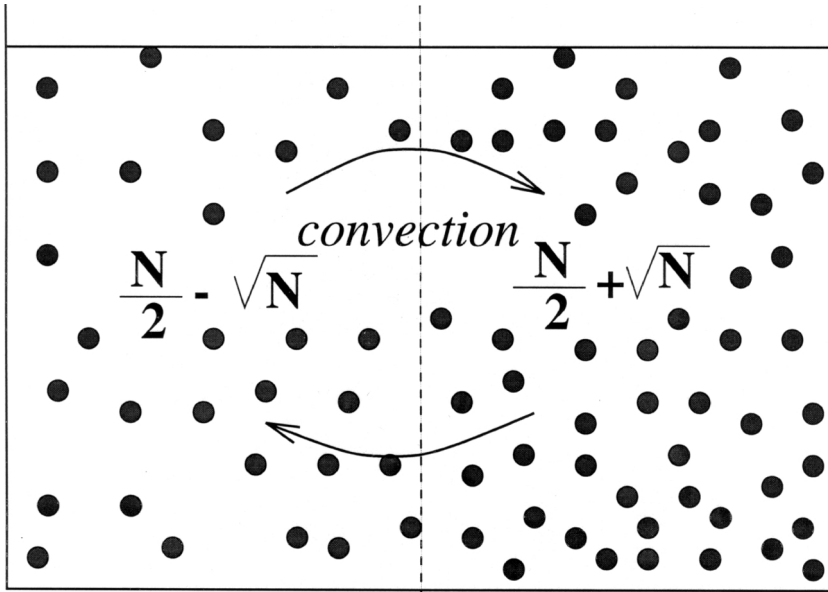


Figure 1. Sketch of the fluctuations in sedimentation.

on the heavy side is $mg \sqrt{N}$, with $m = \frac{4}{3}\pi a^3 \Delta\rho$. Balancing this fluctuation in weight with a Stokes drag $6\pi\mu U'_\ell \ell$ on the velocity fluctuation, and using $U_s = 2\Delta\rho a^2 g/9\mu$, we find the fluctuation in the velocities

$$U'^2_\ell \sim U_s^2 \phi \frac{\ell}{a} \tag{1}$$

With this velocity fluctuation we can estimate the hydrodynamic self-diffusivity as $D_\ell \sim U'_\ell \ell$, corresponding to the particle velocity remaining correlated for a time $\tau_c = O(\ell/U'_\ell)$. Thus,

$$D_\ell \sim aU_s \phi^{1/2} \left(\frac{\ell}{a}\right)^{3/2} \tag{2}$$

This scaling argument helps to explain how velocity fluctuations and hydrodynamic self-diffusivity in a random dilute monodisperse sedimenting suspension depend on the size of the system.

In the simulations we monitored the horizontal variation of density, which is responsible for the convection currents in sedimentation. This is the important origin of the large velocity fluctuations which has not been made clear by previous works (Ladd, 1993, 1997; Koch, 1994) who have worried about Koch and Shaqfeh’s mass deficit theory (1991).

Statement of the Problem

For rigid spherical particles sedimenting in a incompressible Newtonian fluid of dynamic shear viscosity μ and density ρ , with sedimentation velocities sufficiently small to neglect inertial effects, the appropriate equations governing the fluid motion are the pseudo-steady Stokes equations

$$0 = -\nabla P + \mu \nabla^2 \mathbf{u} \quad (3)$$

$$\nabla \cdot \mathbf{u} = 0 \quad (4)$$

where \mathbf{u} and $P = p - \rho \mathbf{g} \cdot \mathbf{x}$ are the velocity and the modified pressure fields. Equations (3) and (4), valid within the fluid, are supplemented by a nonslip boundary condition on the surface of each particle $\mathbf{u} - \mathbf{U}_\alpha + \boldsymbol{\Omega}_\alpha \times (\mathbf{x} - \mathbf{x}_\alpha)$ on $|\mathbf{x} - \mathbf{x}_\alpha| = a$ for $\alpha = 1, 2, \dots, N$. Here \mathbf{U}_α and $\boldsymbol{\Omega}_\alpha$ are, respectively, the velocity and the angular velocity of the sphere α with radius a and center $\mathbf{x}_\alpha(t)$. It should be noted that in a dilute suspension of sedimenting particles the condition for the Stokes equation to be valid is $Re \ll a/\ell^*$, where ℓ^* is the characteristic length scale of the interactions, i.e., the mean interparticle distance. With $\ell^* \sim a\phi^{-1/3}$, the particle Reynolds number must satisfy

$$Re = \frac{\rho a U_s}{\mu} \ll \phi^{1/3}$$

In addition, we consider the limit case where the Péclet number is high, which corresponds to a suspension of non-Brownian particles,

$$Pe = \frac{a U_s}{D} = \frac{6\pi\mu a^2 U_s}{kT} \gg 1$$

where D is the particle diffusivity first derived by Einstein (1956). When the above condition holds, the hydrodynamic forces dominate Brownian motion in determining the suspension microstructure.

Owing to the long range of the velocity disturbance in a dilute sedimenting suspension, we will be interested in particle interactions at separation that are large compared with particle radius. Therefore, with an error $O(\phi)$ in the sedimentation velocity of the particles, the simplest level of point-force approximation may be used to describe the hydrodynamics (Saffman, 1973) with the fluid velocity governed by

$$0 = -\nabla P + \mu \nabla^2 \mathbf{u} + \sum_{\alpha} \mathbf{f}^\alpha \delta(\mathbf{x} - \mathbf{x}_\alpha) \quad (5)$$

Here $\delta(\mathbf{x} - \mathbf{x}_\alpha)$ denotes the Dirac delta function and \mathbf{f}^α is the hydrodynamic force exerted on the fluid by particle α . In the absence of particle

inertia, $\mathbf{f}^\alpha = \frac{4}{3}\pi a_\alpha^3(\rho_\alpha - \rho_f)\mathbf{g}$, which is just the net weight with the buoyancy removed.

We consider sedimentation in a closed container with an impenetrable bottom and vertical walls, for which there is no mean flow at each point of the suspension, i.e., $\langle \mathbf{u} \rangle = 0$. Taking an average of Equation (5), we find an expression for the mean pressure gradient,

$$\langle \nabla P \rangle = \left\langle \sum_\alpha \mathbf{f}^\alpha \delta(\mathbf{x} - \mathbf{x}_\alpha) \right\rangle = n\langle \mathbf{f} \rangle \tag{6}$$

or $\langle P \rangle = n\langle \mathbf{f} \rangle \cdot \mathbf{x}$, which is the global balance for the average pressure gradient, with $\langle \mathbf{f} \rangle = (1/N) \sum_\alpha \mathbf{f}^\alpha$ the average particle force exerted on the fluid. In particular, Equation (6) suggests that in the point-particle approximation the pressure P in Equation (5) may be adjusted to reflect the macroscopic increase in the density of the fluid $\phi\Delta\rho = n|\mathbf{f}|/g$. The pressure is decomposed into a periodic part $p'(\mathbf{x})$ and a linear part $\langle P \rangle$, with gradient given by Equation (6), i.e., $P(\mathbf{x}) = \langle P \rangle + p'(\mathbf{x})$. Substituting the value of the reduced pressure $P(\mathbf{x})$ into Equation (5), one obtains

$$0 = -\nabla p + \mu\nabla^2\mathbf{u} + \sum_\alpha \mathbf{f}^\alpha \delta(\mathbf{x} - \mathbf{x}_\alpha) - n\langle \mathbf{f} \rangle \tag{7}$$

with the following boundary conditions imposed:

$$\begin{cases} u(\mathbf{x}), v(\mathbf{x}), w(\mathbf{x}) & \text{periodic in } x \text{ and } y \text{ directions with period } \ell \\ u(\mathbf{x}), v(\mathbf{x}) & \text{periodic in } z \text{ with period } h \\ w(\mathbf{x}) = 0 & \text{on } z = 0 \text{ and } z = h \end{cases} \tag{8}$$

where u, v , and w are the velocity components of the fluid motion in directions x, y , and z , respectively.

Flow Solution with Impenetrable Boundary

The method of images that plays so important a part in the mathematical theory of elasticity, fluid mechanics, and heat transfer is peculiarly adapted to the solution of the problem of the sedimentation of many interacting particles. The image system used in this work consist of stokeslets equal in magnitude but opposite in sign to the initial stokeslets (Blake, 1971). We construct the appropriate Green's functions for the velocity and pressure field associated with a stokeslet actuating in the gravity direction and satisfying the boundary conditions in Equation (8). Here all components of the velocity field (u, v, w) are periodic in x and y with period ℓ , the horizontal components u and v periodic in z with period h , but with the vertical component w satisfying an impenetrable bottom

and top condition of vanishing vertical velocity. We will show that numerical simulations of point particles sedimenting in a periodic box suggest that an impenetrable lower boundary is important in reducing the vertical-horizontal anisotropy to realistic proportions.

The procedure for obtaining the flow solution within an impenetrable box is essentially to consider a linear combination $\mathbf{u}(\mathbf{x}) = \mathbf{u}(\mathbf{x}; \mathbf{x}_\alpha^s) - \mathbf{u}(\mathbf{x}; \mathbf{x}_\alpha^i)$ that satisfies the governing Equation (7) and the boundary conditions in Equation (8). The first term can be thought as the solution for the periodic flow resulting from an initial stokeslet located at $\mathbf{x}_\alpha^s = (x_\alpha, y_\alpha, z_\alpha)$ within a rectangular box of dimensions $\ell \times \ell \times 2h$ with $u(\mathbf{x}), v(\mathbf{x})$, and $w(\mathbf{x})$ periodic in x and y with period ℓ and u, v , and w periodic in z with period $2h$ (Hasimoto, 1959). The second term corresponds to the fictitious stokeslet of equal magnitude but opposite sign at the image point $\mathbf{x}_\alpha^i = (x_\alpha, y_\alpha, -z_\alpha)$. Using such an image system with Ewald's summation technique in the version of Nijboer and De Wette (Ewald, 1921; Nijboer and De Wette, 1957; Beenakker, 1986; Sangani and Acrivos, 1982), we arrive at the fundamental solution for the Stokes flow induced by a lattice of stokeslets with side periodicity and impenetrable top and bottom. The final result is given by

$$u_j(\mathbf{x}) = \sum_\gamma G_{jm}^{ps}(\mathbf{x} - \mathbf{r}_\alpha^s, \mathbf{x} - \mathbf{r}_\alpha^i) f_m + \frac{1}{V} \sum_\beta J_{jm}^{rs}(\mathbf{k}_\beta) \Theta f_m \tag{9}$$

which has been made dimensionless using a, U_s and $6\pi\mu a U_s$ for the reference scales of length, velocity, and force, respectively.

The kernel tensors G_{jm}^{ps} and J_{jm}^{rs} and the function Θ are defined as follows:

$$G_{jm}^{ps} = J_{jm}^{ps}(\mathbf{x} - \mathbf{r}_\alpha^s) - J_{jm}^{rs}(\mathbf{x} - \mathbf{r}_\alpha^i) \tag{10}$$

$$\Theta = \cos 2\pi \mathbf{k}_\beta \cdot (\mathbf{x} - \mathbf{x}_\alpha^s) - \cos 2\pi \mathbf{k}_\beta \cdot (\mathbf{x} - \mathbf{x}_\alpha^i) \tag{11}$$

where \mathbf{J}_{ps} and \mathbf{J}_{rs} are dimensionless Green's functions in the physical (ps) and reciprocal (rs) spaces, respectively, which conform with the periodicity of the flow (Cunha, 1995)

$$\mathbf{J}^{ps}(\mathbf{r}) = \frac{3}{4} \lambda^{-\frac{1}{2}} \Gamma_{-\frac{1}{2}} \left(\frac{\pi r^2}{\lambda} \right) \mathbf{I} + \frac{3}{2} \pi \lambda^{-\frac{3}{2}} \Gamma_{\frac{1}{2}} \left(\frac{\pi r^2}{\lambda} \right) \mathbf{r}\mathbf{r} \tag{12}$$

$$\mathbf{J}^{rs}(\mathbf{k}) = \frac{3}{2} [\lambda \Gamma_0(\pi k^2 \lambda) \mathbf{I} - \pi \lambda^2 \Gamma_1(\pi k^2 \lambda) \mathbf{k}\mathbf{k}] \tag{13}$$

Here $\mathbf{I} = \delta_{ij} \mathbf{e}_i \mathbf{e}_j$ denotes the unit second-rank tensor, and V is the volume of the periodic box $V = \ell^2 \times 2h$. The wave number vector k is defined as

$\mathbf{k} = (\frac{\beta_1}{\ell}, \frac{\beta_2}{\ell}, \frac{\beta_3}{2h})$, where $\beta_1, \beta_2, \beta_3$ are positive or negative integers $(0, \pm 1, \pm 2, \dots)$. The sums in Equation (9) are performed over a three-dimensional periodic lattice in which each (cell numbered by the index γ) may contain N particles (numbered by the index α). The lattice points are given by the vector $\mathbf{x}_\gamma = (\gamma_1\ell, \gamma_2\ell, \gamma_3 2h)$ with $\gamma_1, \gamma_2, \gamma_3 = 0, \pm 1, \pm 2 \dots$, and a particle has position vector $\mathbf{r}_\alpha = \mathbf{x}_\alpha + \mathbf{x}_\gamma$. \mathbf{x}_α is the position vector of the particle with respect to the origin of its cell. The prime on the reciprocal sum indicates a summation over all reciprocal lattice vectors \mathbf{k} , except where $|\mathbf{k}| = 0$. The exclusion of this term is a direct result of the average pressure balancing the average force the particles exert on the fluid.

The solution for $\mathbf{u}(\mathbf{x})$ given in terms of the sums in Equation (9) converge exponentially fast, with the convergence rate controlled by the arbitrary geometrical parameter $\lambda > 0$. For optimal convergence, λ should be chosen neither too small nor too large. Beenakker (1986) recommends $\lambda = \pi^{1/2} V^{-1/3}$ for simple cubic lattice (i.e., $h/\ell = 1$), giving the equal rates of convergences for the two sums, whereas Cunha (1995) suggests optimum values of the same parameter for anisotropic lattice (i.e., $h/\ell = 2, 3, 4, 5$).

Particle Motion

Now the problem of N spherical particles free of inertia settling within the impenetrable box with periodic sides of dimensions $\ell \times \ell \times h$ is considered. Let \mathbf{x}_α denote the position of the particle α . Suppose an external force \mathbf{f}^α is exerted on particle α , and let \mathbf{U}^α be its translation velocity. Then Equation (9) can be rewritten in an appropriate formulation of hydrodynamic interaction that relates the velocity \mathbf{U}^α and the forces \mathbf{f} as follows:

$$U_i^\alpha = 1 + \sum_\gamma \sum_{m=1}^N G_{ij}^{ps}(\mathbf{r}_\alpha - \mathbf{r}_m) \cdot f_j^m + \frac{1}{V} \sum_\beta \sum_{m=1}^N J_{ij}^{rs}(\mathbf{k}_\beta) \Theta(\mathbf{x}_\alpha - \mathbf{x}_m) \cdot f_j^m \quad (14)$$

with particle trajectories being obtained by integration of the kinematics equation

$$\frac{dx_i^\alpha}{dt} = U_i^\alpha, \quad x_i^\alpha(0) = x_o^\alpha \quad (15)$$

Here $\mathbf{f}^m = -\frac{2}{9\mu} a^2 \frac{\Delta\rho}{U_s} \mathbf{g} = (0, 0, 1)$. The prime on the first sum means that the term $\alpha = m$ in cell $\gamma = 1$ has been excluded.

Equations (14) and (15) will be applied to examine the dynamics of N point particles sedimenting and interacting hydrodynamically within a container of impenetrable boundaries. This type of formulation represents

a mobility problem with hydrodynamic interactions $O(N^2)$, calculated by using pairwise additivity (i.e., superposition of velocity) in the mobility matrix. We emphasize that our purpose here is not to perform detailed calculations of particle interactions. Rather, we aim to explore the physical processes giving rise to velocity fluctuations and their consequence when particles sediment. It will be shown next that point particle interactions suffice for the production of random particle migration needed to reproduce the phenomenon of hydrodynamic dispersion.

COMPUTER SIMULATIONS

A numerical routine was constructed to compute the horizontal number density fluctuations and velocity fluctuations and to examine the long time of the fluctuating particle motion in the suspension. To meet these ends, the numerical studies of the suspension were carried out in two stages. First, macroscopic properties of the particles' motion were evaluated over a 100 different initial configurations of the particles within the container (i.e., at time = 0). The main goal was to verify the scaling arguments presented at the beginning of this article, which predict variance of the sedimentation velocity increasing with the linear size of the box.

The time evolution of the system was analyzed over 10 realizations. The main problem that we examined was to see how the initial configurations of the particles evolve in time. The velocity autocorrelation functions, the hydrodynamic self-diffusivities, and the correlation times in the direction parallel and perpendicular to gravity were determined. More importantly, the ratios $\langle U_{\parallel}^2 \rangle / \langle U_{\perp}^2 \rangle$, $D_{\parallel} / D_{\perp}$ and $t_{\parallel} / t_{\perp}$, as a function of the box parameter $\phi\ell/a$, for indicating the amount of anisotropy of the dispersion process were calculated. Here the indices \parallel and \perp denote, respectively, quantities parallel and perpendicular to gravity with the dimensionless variances of the sedimentation velocity and the hydrodynamic self-diffusivities expressed in tensorial forms as follows:

$$\langle \mathbf{U}'\mathbf{U}' \rangle = \langle U_{\parallel}^2 \rangle \mathbf{e}_z \mathbf{e}_z + (\mathbf{I} - \mathbf{e}_z \mathbf{e}_z) \langle U_{\perp}^2 \rangle$$

and

$$\mathbf{D} = \mathbf{e}_z \mathbf{e}_z D_{\parallel} + (\mathbf{I} - \mathbf{e}_z \mathbf{e}_z) D_{\perp}$$

In order to accelerate the calculations of Ewald summations and thereby obtain considerable savings in computer time, the incomplete gamma functions were then tabulated for the values of $\nu = (-1/2, 0, 1/2, 1)$, and the calculation required for each particle pair interaction

was determined by simple linear interpolation from these tables. An important step of the preliminary tests was investigating the link-parameter λ between the physical and reciprocal spaces. Since we have performed simulations with different aspect ratios $h/\ell (= 2, 3, 4, 5)$, it was desirable to investigate the optimum values of λ that correspond to the maximum value of the solution when using a relatively small number of boxes. The integration of Equation (15) via a fourth-order Runge-Kutta scheme provided the instantaneous position of the particle's motion, with \mathbf{U}^i being evaluated at each time step by means of Equation (14). The magnitude of the time step Δt in the Runge-Kutta procedure was set up as $\Delta t \sim a/U_s$ (that is, the time taken for a single particle to fall across its own radius; the Stokes time). The horizontal components of the particle velocity were seen to be null (i.e., no fluctuations in the particle's trajectory since there are no neighboring particles), and the vertical component persisted constant until the particle got in the region of influence of the image system (the finite effect of the box). At the bottom the particle completely stopped its settling motion. This information was essential to define a bulk region of the suspension in which the statistical data analysis should produce meaningful statistics. Thus we hold that during the calculation of the transport properties of the suspension the statistical data analysis is evaluated in a region of the box where the variations in the individual velocity of a reference particle are due only to its interaction with neighboring particles.

Some information was needed to start the computation of particles' trajectory in the simulation. Here the simulations all started at $t = 0$, with the particles located randomly and independently within the impenetrable container. This kind of configuration was generated by the hypothetical process of choosing the positions of the particle's centers one by one at random in $\mathcal{V} = \ell^2 h$, obeying the rule, however, that the center of one sphere cannot be located within an excluded volume shell $a < r < 2a$ of any other sphere. This process is equivalent to excluding the configurations for which overlapping of spheres occurs, with all allowed configurations having equal probability. The statistics routine in our computer simulation program included calculations of the horizontal density fluctuation, sedimentation velocity and its variances parallel and perpendicular to the gravity direction, the velocity auto-correlation functions, the hydrodynamic self-diffusivities, and correlation times.

Statistical Analysis of the Simulations

The horizontal fluctuations in the density of the suspension are the origin of the large convection currents during sedimentation. We investigate the

magnitude of these fluctuations by constructing the Fourier amplitude for the lowest mode in the x -direction of the number density

$$\langle n_{\perp}^2 \rangle = \sum_{j,k} e^{2\pi i(x_j - x_k)/\ell} \quad (16)$$

summing over the differences in the x -coordinates of the positions of the particles.

The instantaneous mean of the velocities of the sedimenting particles is

$$\overline{\mathbf{U}(\mathbf{t})} = \frac{1}{N} \sum_{i=1}^N \mathbf{U}_i(\mathbf{t}) \quad (17)$$

We measure the fluctuations in the velocities with the instantaneous variance

$$\langle U'^2(t) \rangle = \frac{1}{N-1} \sum_{i=1}^N (U_i(t) - \overline{U}(t))^2 \quad (18)$$

constructed for the vertical and two horizontal components of velocity, the variances of the horizontal components then being averaged to give $\langle U_{\parallel}'^2 \rangle$ and $\langle U_{\perp}'^2 \rangle$.

The persistence in time of the velocity fluctuations is investigated using the autocorrelation function, which correlates the velocity at time t with itself at the initial instant,

$$\langle U'(t)U'(0) \rangle = \frac{1}{N-1} \sum_{i=1}^N (U_i(t) - \overline{U}(t))(U_i(0) - \overline{U}(0)) \quad (19)$$

This again is constructed for the vertical and two horizontal components, with the horizontal components afterwards averaged together. We shall report these autocorrelation functions normalized by the variances, i.e.,

$$C_{\parallel}(t) = \frac{\langle U'(t)U'(0) \rangle}{\langle U'(0)U'(0) \rangle} \quad (20)$$

and similarly for $C_{\perp}(t)$.

The random motion of the sedimenting particles can be characterized by a diffusion process with diffusivity calculated as the integral over time of the velocity autocorrelation function

$$D = \int_0^{\infty} \langle U'(t)U'(0) \rangle dt \quad (21)$$

again constructed for the vertical D_{\parallel} and averaged over the two horizontal directions for D_{\perp} . An important question is whether this integral converges at long times: if it does not, the diffusion process is anomalous. The ratio of the diffusivities to the velocity variance gives the integral time-correlation $T^c = D/\langle U'^2 \rangle$.

Here the angle brackets denote a sum over all particles, and an average over all configurations or realizations (i.e., an average over time in dynamic simulation).

RESULTS

Initial Configurations

Several cases were studied. The particle concentration was varied through the range $0 < \phi < 3\%$. Three different box sizes were studied, with $a/\ell = 0.05, 0.06,$ and 0.07 . The aspect ratio of the box was kept constant at $h/\ell = 3$. For each case, 100 different initial configurations were generated by positioning the particles randomly and independently except for not overlapping. The initial velocities were then calculated for each configuration.

First we examined the mean velocity. The mean horizontal velocity $\langle U_{\perp} \rangle$ was found to be zero, a check on our coding. The mean vertical velocity $\langle U_{\parallel} \rangle$ was found to be in agreement with $U_s (1 - 5.5\phi)$, the prediction of Batchelor (1972) for point particles (see Figure 2). The small degree of scatter suggests that some of the initial random configurations accessible through our simulations were not perfectly statistically homogeneous (i.e., configurations with uniform probability), as assumed by Batchelor's analysis. This hindering of the settling is due to a back flow outside the particle, which occurs since we imposed the condition of no mean flow, $\langle \mathbf{u} \rangle = 0$.

Figure 3 illustrates how the simulations were analyzed for the case $\phi = 2\%$ and $a/\ell = 0.05$, in which we used $N = 114$ particles. For each of the 100 realizations, we computed the initial value of the horizontal density fluctuation $\langle n_{\perp}^2 \rangle$ and the initial value of the fluctuations in the vertical and horizontal velocities $\langle U_{\parallel}^{\prime 2} \rangle$ and $\langle U_{\perp}^{\prime 2} \rangle$. The horizontal lines in Figure 3 denote the averages across the 100 realizations.

The horizontal density fluctuation divided by N has a value in Figure 3 close to the theoretical value of unity, indicating that the numerical process of positioning the particles has produced a well-stirred suspension with the standard $\pm\sqrt{N}$ statistical fluctuations.

The fluctuations in Figure 3 of the vertical velocity are large, just smaller than the mean sedimentation velocity. This is in good general agreement with the experiments (Ham and Homay, 1988) where the fluctuations ranged between 25% and 46% of the mean in the dilute

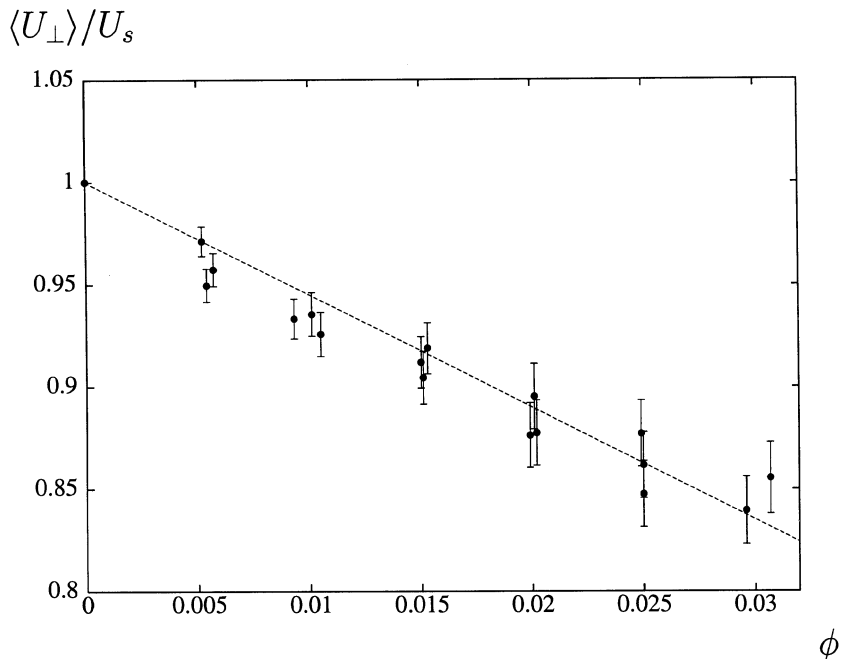


Figure 2. Dimensionless mean settling velocities of the particles calculated over 100 random and independent configurations as a function of the particle concentration. The points with error bars on the graphics correspond to three different aspect ratios a/L used in the computer simulations, and the solid curve is the theoretical result of Batchelor (1972) $(1 - 5.5\phi)$, for a dilute homogeneous suspension of point particles.

suspensions. Our results are also in good general agreement with the experiments of Nicolai et al. (1995), who found a relative fluctuation of 77% at $\phi = 5\%$. The theoretical value of Koch and Shaqfeh (1991) gives a slightly higher value of $\sqrt{\langle U_{\parallel}^2 \rangle} = 2.2U_s$.

The ratio in Figure 3 of the vertical to horizontal velocity fluctuations was found to be 2.5, indicating a strong anisotropy. This is close to the experiment value of 2 found by Nicolai et al. (1995), and close to the ratio of 3 found by theory and numerical simulations (Ladd, 1993; Koch, 1994).

The results in Figure 3 are for a single case of $\phi = 2\%$ and $a/l = 0.05$. We now consider results for different particle concentrations and box sizes. The origin of the large scale velocity fluctuations is the convection caused by the horizontal density fluctuation $\langle n_{\perp}^2 \rangle$. We collect together in Figure 4 its average over the 100 realizations in each of the 18 different cases studied. Although the results are plotted as a function of the number of particles used in the different cases, we see that the

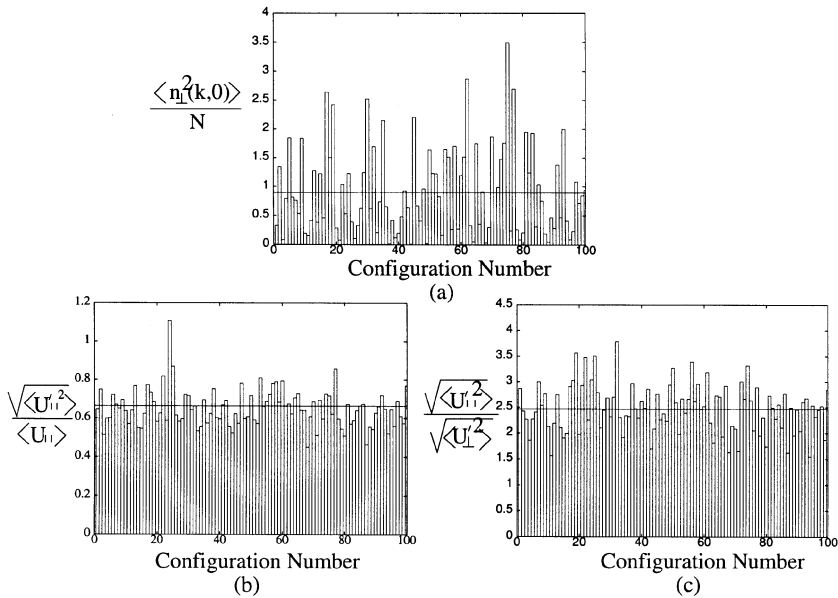


Figure 3. Results of the numerical simulations at time=0 with statistics over 100 random and independent distribution of particles in the impenetrable box. The aspect ratios $h/\ell = 3$, $a/\ell = 0.05$, and the number of sedimenting particles was equal to 114, corresponding to a volume concentration of 2%. \parallel and \perp denotes the directions parallel and perpendicular to gravity, respectively. (a) horizontal density number fluctuation; (b) vertical relative velocity fluctuation; (c) ratio between the vertical and horizontal fluctuations.

horizontal density fluctuations are essentially constant, equal to the standard $\pm\sqrt{N}$ statistical fluctuation.

Finally, in Figures 5 and 6 we examine the variation of the fluctuations in the vertical and horizontal velocities. The results for the cases with different particle concentrations ϕ and box sizes a/ℓ are plotted against the expected scaling parameter $\phi\ell/a$. We see that both variances increase linearly with the size of the box, with linear fits $\langle U_{\perp}^{\prime 2} \rangle = 0.029U_s^2\phi\ell/a$ and $\langle U_{\parallel}^{\prime 2} \rangle = 0.178U_s^2\phi\ell/a$. Thus, in agreement with Cafisch and Luke (1985) and Hinch (1988), we conclude that when the particles are positioned randomly, initially there are velocity fluctuations proportional to the size of the box.

Time Evolution

A typical evolution of the suspension as it sediments is given in Figure 7. This figure is for one realization of the case of a particle concentration

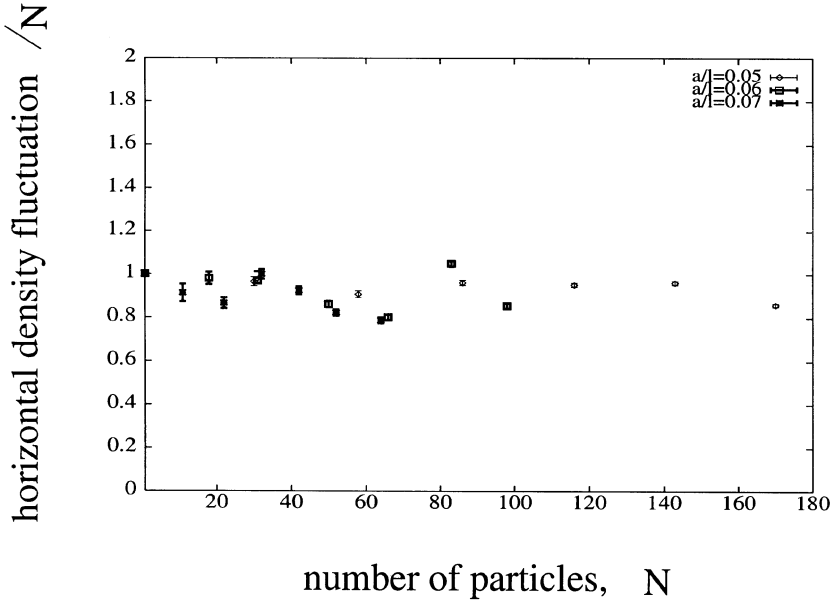


Figure 4. Dimensionless horizontal density fluctuation obtained over 100 random and independent configurations as a function of the number of particles.

$\phi = 5\%$, a box size of $a/\ell = 0.05$, and an aspect ratio of the box $h/\ell = 3$, a simulation requiring $N = 286$ particles. We show at six different times the positions of the particles projected onto the vertical xz -plane. The first time is the initial configuration with the particles distributed randomly inside the box. As time progresses, a sediment accumulates on the lower impenetrable boundary. Note that the impenetrable boundary is slippery and not a no-slip rigid boundary, so that particles can be seen moving along it. The descending upper interface between the suspension and clear fluid above is diffuse and spreads slowly, so that the nearby concentration of particles decreases in time.

For each case studied, dynamic simulations were made for 10 realizations with different initial configurations. Below we give only averages over the 10 realizations. Moreover, in calculating the averages, we select the middle part of the suspension, away from the sediment and the diffuse upper front.

Figure 8 shows the time evolution of the horizontal density fluctuations for five different combinations of particle concentrations and box size. In each of the five different cases studied, the horizontal density fluctuations are seen to remain essentially constant up to $t = 20a/U_s$, approximately the time to fall through the width of the box

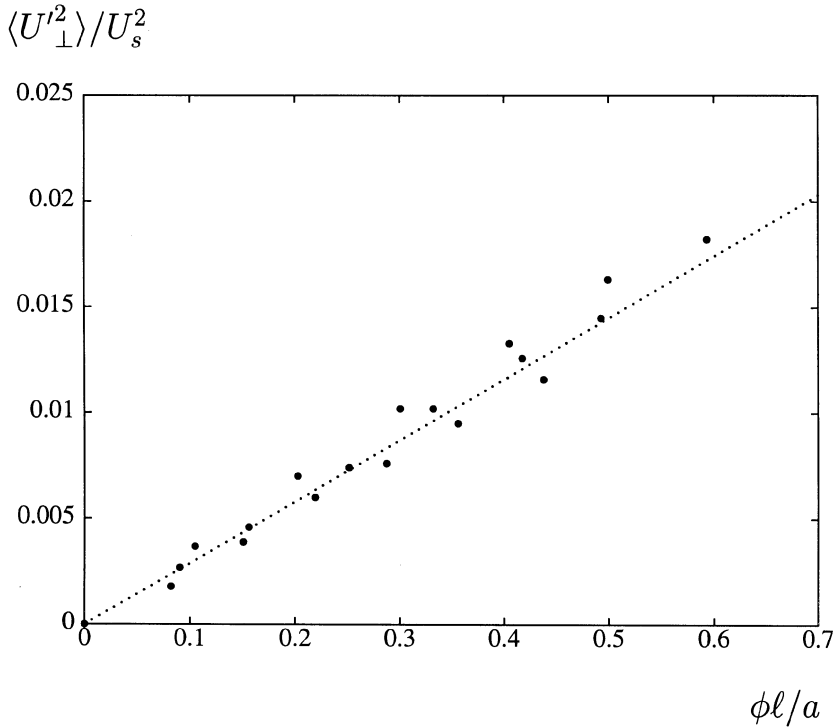


Figure 5. Dimensionless variance of the mean settling velocity of the particles, perpendicular to the gravity, as a function of the system parameter $\phi\ell/a$. The dotted line is the linear fit $\langle U_{\perp}'^2 \rangle / U_s^2 = 0.029 \phi(\ell/a)$.

ℓ or one-third the time to fall the height of the box h . We had expected that during such a time the density fluctuations would drive a convection that would turn the horizontal variations in density into vertical variations, and so the large velocity fluctuations would decay. Our dynamic simulations show, however, that the convection does not lead to a systematic decrease in the horizontal density fluctuations. Further simulations (Cunha, 1995) with a taller box, $h/\ell = 4$, found the same behavior.

Corresponding to the lack of evolution of the density fluctuations in Figure 8, Figure 9 shows that the horizontal and vertical velocity fluctuations also remain constant in time. They therefore remain proportional to the size of the box, as in the parameter $\phi\ell/a$, and do not evolve to some value that is independent of the size of the box. The computer simulations therefore remain at variance with experimental observations of fluctuations independent of the size of the box.

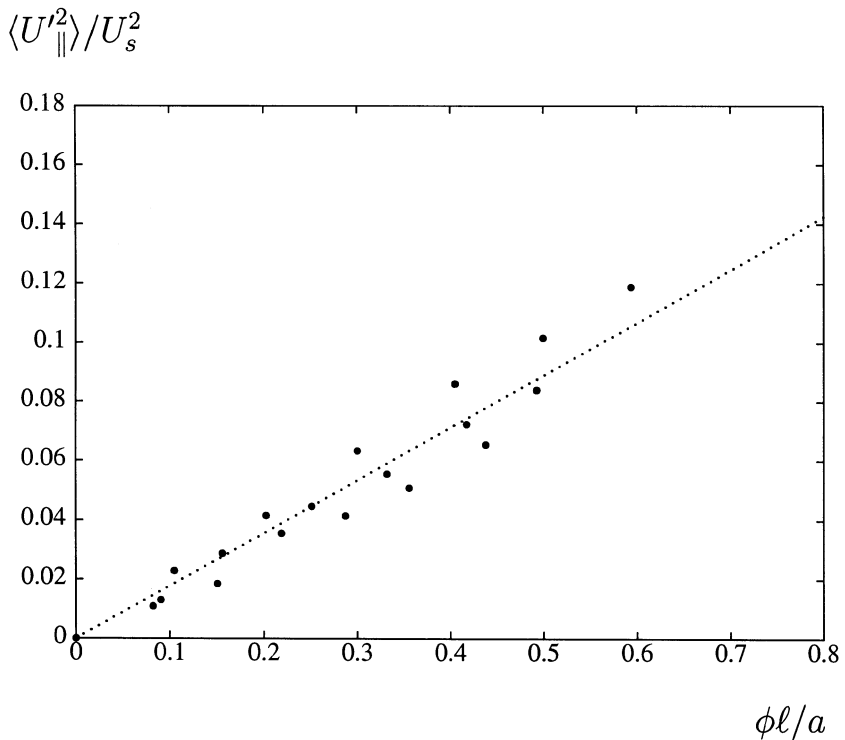


Figure 6. Dimensionless variances of the mean settling velocity of the particles, parallel to the gravity, as a function of the system parameter $\phi \ell / a$. The dotted line is the linear fit $\langle U_{\parallel}^2 \rangle / U_s^2 = 0.178 \phi(\ell/a)$.

The velocities of the particles fluctuate randomly in time, apparently with a magnitude that does not evolve during the sedimentation. We study the random variation by examining the autocorrelation function of the velocity, in which the velocity is correlated with itself at various time delays. Figure 10 gives the autocorrelation function, nondimensionalized by the variance (correlation with zero time delay), for the horizontal and vertical velocity, both for our computer simulations in the case $\phi = 3\%$, $a/\ell = 0.05$, and $h/\ell = 3$ and for the experiments of Nicolai et al. (1995) in the case $\phi = 5\%$, $a/\ell = 0.01$, $h/\ell = 10$, and $w/\ell = 2.5$. There is good general agreement in which the velocities lose correlation over a time of $O(10a/U_s)$ and the vertical velocity decorrelates slightly faster.

The integral over time of the velocity autocorrelation function gives the self-diffusivities of the random walk of the particles as they sediment. Figure 11 shows the time integral increasing to its asymptotic value on

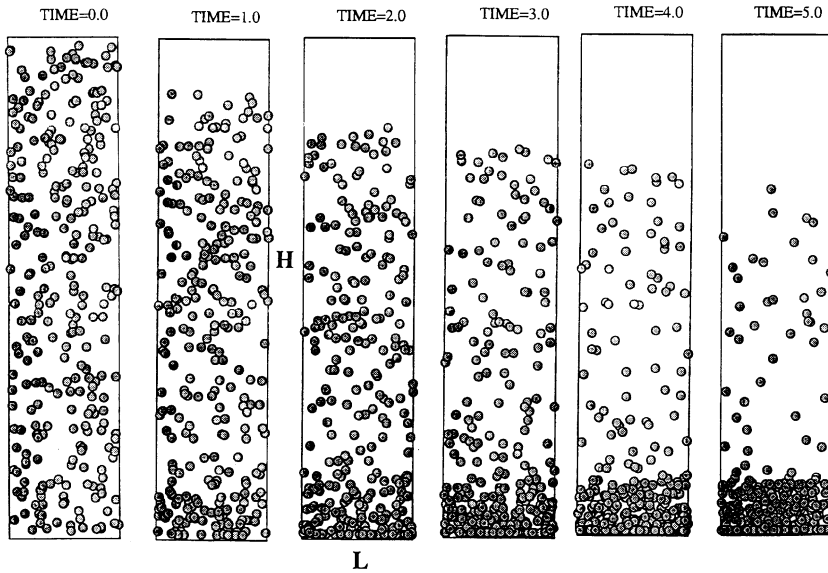


Figure 7. A typical picture of the dynamical simulations of the sedimenting suspension studied for $a/\ell = 0.05$, $h/\ell = 3$, $N = 286 \Rightarrow \phi = 5\%$.

the correlation time of $O(10a/U_s)$. For the case $\phi = 3\%$, $a/\ell = 0.05$, and $h/\ell = 3$ we find a diffusivity in the direction of gravity $D_{\parallel} = 2aU_s$. This value should be compared with the experimental values of Ham and Homsy (1988) increasing from $2aU_s$ at $\phi = 2.5\%$ to $6aU_s$ at $\phi = 6\%$, and the experimental value of Nicolai et al. (1995) around $5aU_s$. Hydrodynamic screening theory gives $D_{\parallel} = 0.52aU_s/\phi$, i.e., the larger value $17aU_s$ at $\phi = 3\%$ (Koch and Shaqfeh, 1991).

Figure 12 shows our results for the self-diffusivity parallel to gravity as a function of the scaling parameter $\phi^{1/2}(\ell/a)^{3/2}$. The results for various particle concentrations ϕ and box sizes a/ℓ can be approximated by the linear fit $D_{\parallel} = 0.19aU_s\phi^{1/2}(\ell/a)^{3/2}$. While the values of the diffusivity are comparable with those in laboratory experiments, a direct comparison is not possible because our simulations depend on the size of the box and the laboratory experiments do not.

The random fluctuations during sedimentation exhibit considerable anisotropy. In Figure 12 we give the ratio of the vertical to horizontal rms velocity fluctuations as a function of the scaling parameter $\phi\ell/a$. We find the ratio is essentially constant at $\sqrt{\langle U_{\parallel}^{\prime 2} \rangle} / \sqrt{\langle U_{\perp}^{\prime 2} \rangle} \approx 2.5$. This value is similar to that found in experiments by Nicolai et al. (1995) and in numerical simulations (Leighton and Acrivos, 1987; Koch, 1994). We also present in Figure 13 our results for the ratio of the vertical to horizontal

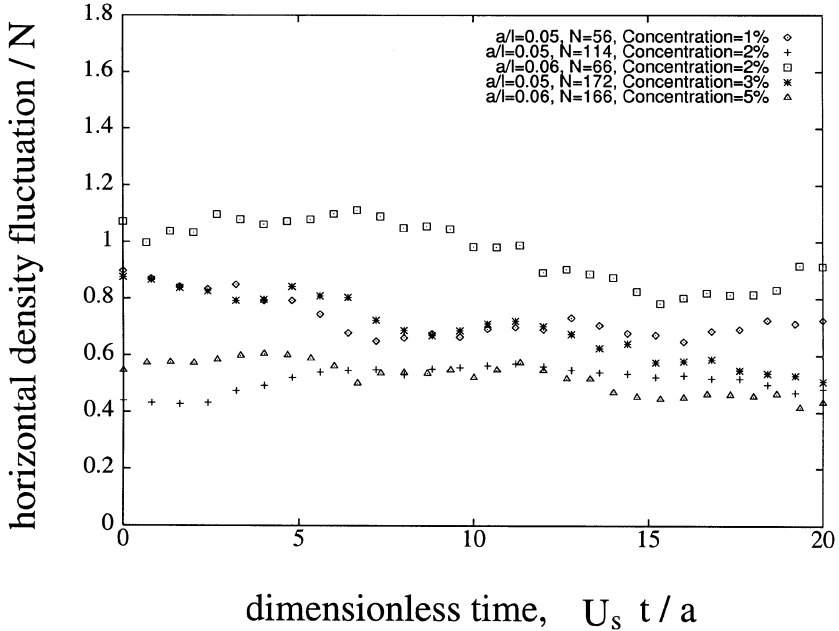


Figure 8. Results of the computer simulations for the time development of the dimensionless horizontal density number fluctuation at different conditions of the simulated system with the aspect ratio $h/\ell = 3$.

self-diffusivities. We find that $D_{\parallel}/D_{\perp} \approx 10$ in all our simulations. This should be compared with a value around 5 in the experiments of Nicolai et al. (1995), and a value $O(100)$ in the simulations by Ladd (1993) and Koch (1994). Koch found that he could reduce this figure to around 25 by increasing the aspect ratio of his box from $h/\ell = 1$ to $h/\ell = 3$. We speculate that this still high value results from the use of a full periodic boundary condition in the vertical rather than our impenetrable boundary condition.

Since completing the work reported here (Cunha, 1995), the lattice-Boltzmann simulations of Ladd (1997) have come to our attention. Ladd reported numerical results of fluctuations and hydrodynamic dispersion in sedimentation for a large homogeneous suspension using 32768 particles ($\phi = 10\%$) at finite Reynolds number ($Re_W = 0.45$), based on width of the periodic cell. His results show an anisotropy in velocity fluctuations about 2.7 and an anisotropy in correlation time equal to 2.5 that agree well with our numerical results and experiments. However, the ratio of diffusivities equal to 23 for $h/l = 4$ are larger than the result here and about five times the experimental measurements. Our results suggest that

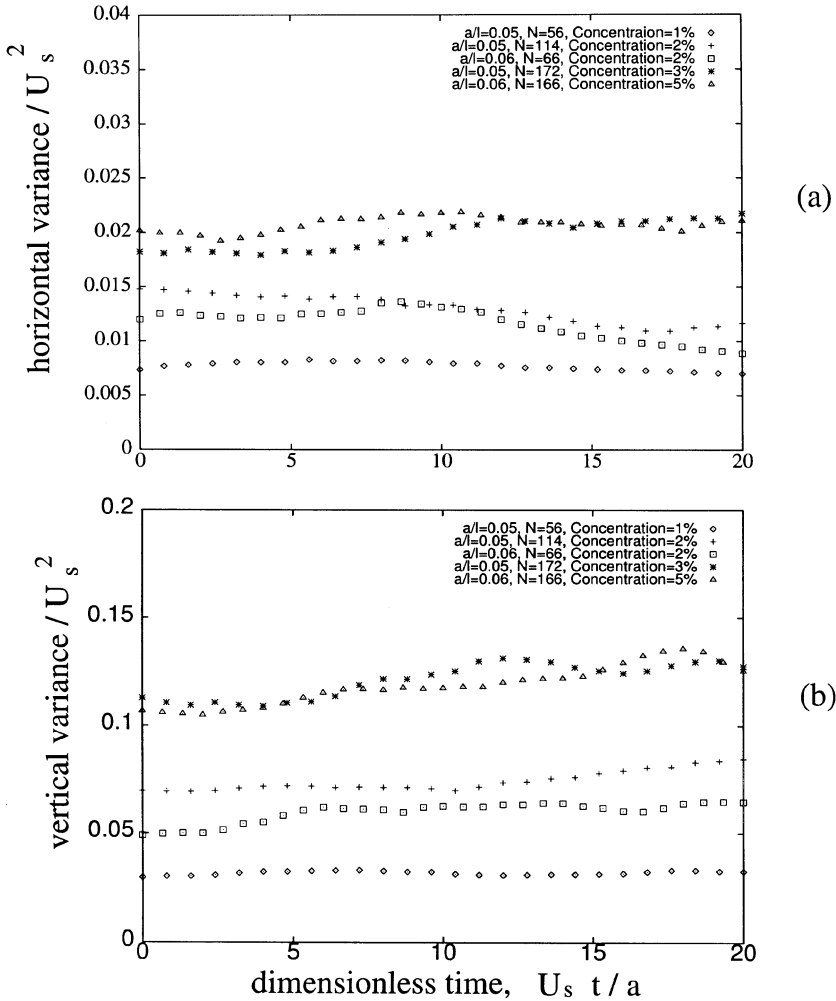


Figure 9. Results of the computer simulations for the time development of the dimensionless variances, both perpendicular to gravity (a) and parallel to gravity (b) for different conditions of the simulated system with the aspect ratio $h/\ell = 3$.

simulations for a finite height of suspension approaching a no-flux boundary with periodic boundary conditions in the horizontal direction permit better capturing of the anisotropic nature of the particle interactions. Surprisingly, these large system simulations for finite Reynolds numbers closely follow our results, showing the same system size dependence in velocity fluctuations, $O((\ell/a)^{1/2})$ and hydrodynamic diffusivities $O((\ell/a)^{3/2})$, which do not agree with the experimental results of

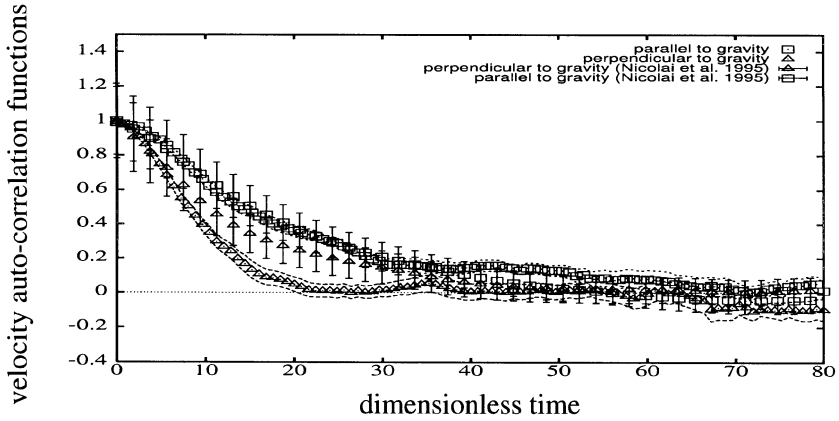


Figure 10. Normalized velocity fluctuation autocorrelation functions parallel and perpendicular to the gravity direction. Computer simulations for $h/\ell = 3$, $a/\ell = 0.05$, $N = 172 \Rightarrow \phi = 3\%$. The error bars represent experimental data (Nicolai et al. 1995) with $\phi = 5\%$, $h/\ell = 4$, $h/w = 10$, and $w/a \approx 100$. The dashed lines indicate the uncertain range of the present computer simulations.

Nicolai and Guazzelli (1995). Ladd also leaves open the question about the existence of a hydrodynamic screening for a random dilute mono-disperse suspension in the way of the mass deficit predicted by Koch and Shaqfeh's theory (1991).

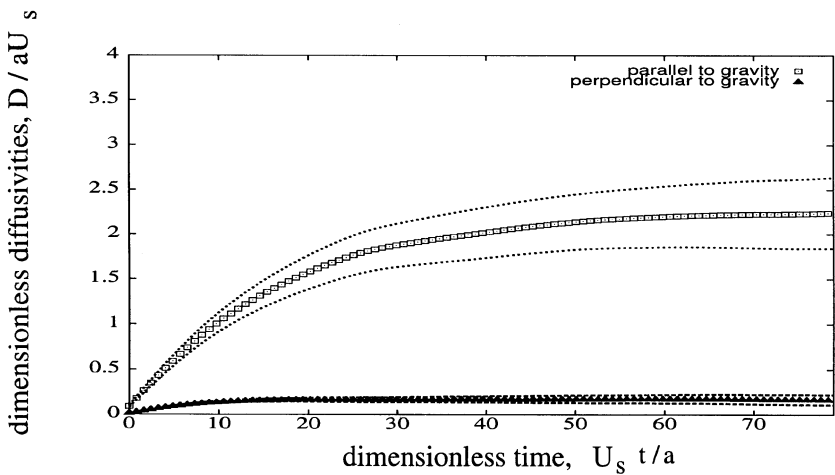


Figure 11. Dimensionless hydrodynamic self-diffusivities for $h/\ell = 3$, $a/\ell = 0.05$, and $\phi = 3\%$. The dashed lines are the error bars.

$$D_{\parallel} / aU_s$$

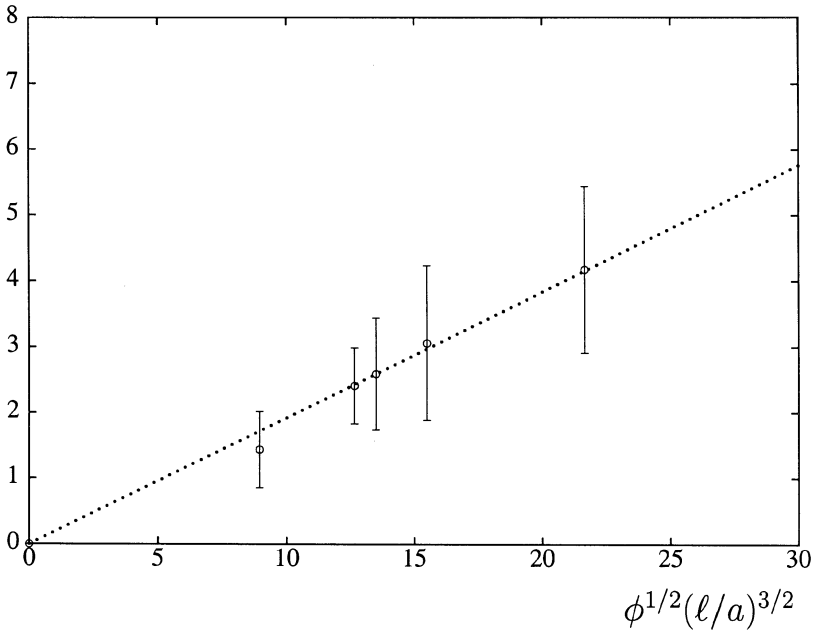
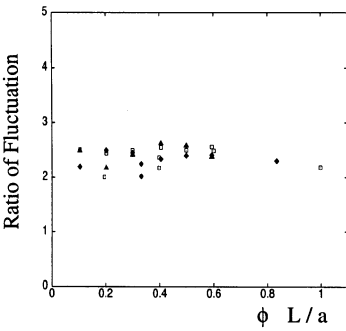
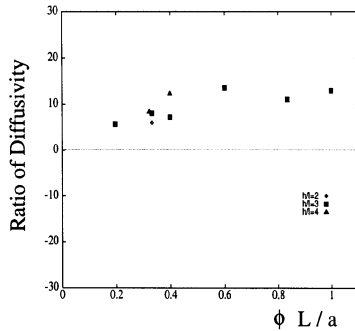


Figure 12. Vertical dimensionless hydrodynamic self-diffusivity as a function of the scaling $\phi^{1/2}(\ell/a)^{3/2}$. The dotted line is the linear fit $D_{\parallel} = 0.19 aU_s \phi^{1/2}(\ell/a)^{3/2}$.



(a)



(b)

Figure 13. Ratio of anisotropy calculated during all the computer simulations. (a) degree of anisotropy in velocity fluctuations, (b) in self-diffusivities.

CONCLUSIONS

Direct numerical simulations of a monodisperse dilute suspension of point particles with excluded volume sedimenting at low Reynolds number in a rectangular box with periodic sides and impenetrable bottom and top have been used to describe the microstructure, velocity fluctuations, and dispersion of such suspension. The numerical results reveal fluctuations in the velocity of individual particles as being due to varying configuration of neighboring particles and resulting hydrodynamic interactions between the suspended particles. The evolution of the positions of the particles was investigated in a finite container. In particular, the large fluctuations that occur in sedimentation when inertia is very small do not decay in time when the initial particle configurations are random with no overlappings. Our numerical computations have found velocity fluctuations and hydrodynamic self-diffusivity increasing in a predictable way with the system size that agrees with scaling arguments, with theory, and with recent large-scale lattice-Boltzmann simulations, but experiments find differently. We may conclude that the dispersion process in these simulations was controlled by convective motions that scaled with the size of the simulation cell.

The simulations showed degree of anisotropy in velocity fluctuations, correlation times, and hydrodynamic self-diffusivities independent of the system size, and in close agreement with experimental measurements. The normalized autocorrelation functions in both parallel and perpendicular directions to gravity also agreed well with those predicted experimentally for dilute suspension.

While the average velocity in sedimentation can be successfully predicted theoretically, we are still unable to predict and to renormalize the rms fluctuations. Since experimental systems are never perfectly statistically homogeneous and the actual particle distribution is unknown, more work should be done investigating the difference between placing the particles at random and independently in the computer simulations and the procedure of stirring the suspension in the laboratory. Certainly, the development of new numerical simulations including the effects of the container walls, the full multiparticle hydrodynamic interactions, and polydispersity would be important and challenging to explain the experimental results.

ACKNOWLEDGEMENTS

FRC acknowledges the financial support from CNPq-Brasília/Brazil. Computing facilities were provided by the SERC Computational Science Initiative Grant GR/H57585, and an additional grant from the DTI LINK programme on Colloids. We wish to thank Elizabeth Guazzelli

(LPMH/ESPCI, Paris) for kindly providing the experimental data plotted in Figure 10.

REFERENCES

- Batchelor, G. K. (1972). *J. Fluid Mech.*, **240**, 651.
- Beenakker, C. W. J. (1986). *J. Chem. Phys.*, **85**, 1581.
- Blake, J. R. (1971). *J. Fluid Mech.*, **70**, 303.
- Cafisch, R. E. and Luke, H. C. (1985). *Phys. Fluids*, **28**, 759.
- Cunha, F. R. (1995). *Hydrodynamic Dispersion in Suspensions*. Ph.D. thesis Department of Applied Mathematics and Theoretical Physics, Cambridge University.
- Cunha, F. R. (1997). *J. Braz. Soc. Mechanical Sci.*, **19**(4), 474.
- Cunha, F. R. and Hinch, E. J. (1996). *J. Fluid Mech.*, **309**, 211.
- Davis, R. H. (1996). *J. Fluid Mech.*, **310**, 325.
- Davis, R. H. and Hassen, M. A. (1988). *J. Fluid Mech.*, **196**, 107. Corrigendum, (1989). *J. Fluid Mech.*, **202**, 598.
- Einstein, A. (1956). *Investigations on the Theory of the Brownian Movement*. Garden City, NY: Dover Publications.
- Ewald, P. P. (1921). *Ann. Phys. Lpz.*, **64**, 253.
- Ham, J. M. and Homsy, G. M. (1988). *Int. J. Multiphase Flow*, **14**, 553.
- Hasimoto, H. (1959). *J. Fluid Mech.*, **5**, 317.
- Hinch, E. J. (1988). In: *Disorder and Mixing*, ed. E. Guyon, J. P. Nadal, and Y. Pomeau, Dordrecht, The Netherlands: Kluwer, 153.
- Koch, D. L. (1992). *Phys. Fluids*, **4**, 1337.
- Koch, D. L. (1993). *Phys. Fluids*, **5**, 1141.
- Koch, D. L. (1994). *Phys. Fluids*, **6**, 2894.
- Koch, D. L. and Shaqfeh, E. G. (1991). *J. Fluid Mech.*, **224**, 275.
- Ladd, A. J. C. (1993). *Phys. Fluids*, **5**, 299.
- Ladd, A. J. C. (1997). *Phys. Fluids*, **9**, 491.
- Lee, S., Jang, Y., Choi, C. and Lee, T. (1992). *Phys. Fluids*, **4**, 2601.
- Leighton, D. T. and Acrivos, A. (1987). *J. Fluid Mech.*, **181**, 415.
- Nicolai, H. and Guazzelli, E. (1995). *Phys. Fluids*, **7**, 3.
- Nicolai, H., Herzhaft, B., Hinch, E. J., Oger, L. and Guazzelli, E. (1995). *Phys. Fluids*, **7**, 12.
- Nijboer, B. R. A. and De Wette, F. W. (1957). *Physica*, **23**, 309.
- Saffman, P. G. (1973). *Stud. Appl. Math.*, **52**, 115.
- Sangani, A. S. and Acrivos, A. (1982). *J. Multiphase Flow*, **8**, 343.
- Ségre, P. N. Herbolzheimer, E. and Chaikin, P. M. (1997). *Phys. Rev. Lett.*, **79**, 2574.
- Xue, J.-Z., Herbolzheimer, E., Rutgers, M. A., Russel, W. B. and Chaikin, P. M. (1992). *Phys. Rev. Lett.*, **69**, 1715.

Copyright of Chemical Engineering Communications is the property of Taylor & Francis Ltd and its content may not be copied or emailed to multiple sites or posted to a listserv without the copyright holder's express written permission. However, users may print, download, or email articles for individual use.